

See discussions, stats, and author profiles for this publication at: <https://www.researchgate.net/publication/43147546>

# Membrane solubilisation and reconstitution by octylglucoside: Comparison of synthetic lipid and natural lipid extract by isothermal titration calorimetry

ARTICLE *in* BIOPHYSICAL CHEMISTRY · MARCH 2010

Impact Factor: 1.99 · DOI: 10.1016/j.bpc.2010.03.013 · Source: PubMed

---

CITATIONS

11

---

READS

47

3 AUTHORS, INCLUDING:



[Sandro Keller](#)

Technische Universität Kaiserslautern

89 PUBLICATIONS 1,297 CITATIONS

SEE PROFILE



# Membrane solubilisation and reconstitution by octylglucoside: Comparison of synthetic lipid and natural lipid extract by isothermal titration calorimetry

Oxana O. Krylova<sup>a</sup>, Nadin Jahnke<sup>a</sup>, Sandro Keller<sup>a,b,\*</sup>

<sup>a</sup> Leibniz Institute of Molecular Pharmacology (FMP), Robert-Rössle-Str. 10, 13125 Berlin, Germany

<sup>b</sup> Molecular Biophysics, University of Kaiserslautern, Erwin-Schrödinger-Str. 13, 67663 Kaiserslautern, Germany

## ARTICLE INFO

### Article history:

Received 29 January 2010

Received in revised form 12 March 2010

Accepted 13 March 2010

Available online 20 March 2010

### Keywords:

Detergent

Liposome

Micelle

Partition coefficient

Phase diagram

Vesicle

## ABSTRACT

We have studied the solubilisation and reconstitution of lipid membranes composed of either synthetic phosphatidylcholine or *Escherichia coli* polar lipid extract by the non-ionic detergent octylglucoside. For both lipid systems, composition-dependent transformations of unilamellar vesicles into micelles or *vice versa* were followed by high-sensitivity isothermal titration calorimetry. Data obtained over a range of detergent and lipid concentrations could be rationalised in terms of a three-stage phase separation model involving bilayer, bilayer/micelle coexistence, and micellar ranges, yielding the detergent/lipid phase diagrams and the bilayer-to-micelle partition coefficients of both detergent and lipid. The most notable difference between the lipids investigated was a substantial widening of the bilayer/micelle coexistence range for *E. coli* lipid, which was due to an increased preference of the detergent and a decreased affinity of the lipid for the micellar phase as compared with the bilayer phase. These effects on the bilayer-to-micelle partition coefficients could be explained by the high proportion in *E. coli* membranes of lipids possessing negative spontaneous curvature, which hampers both their transfer into strongly curved micellar structures as well as the insertion of detergent into condensed bilayers.

© 2010 Elsevier B.V. All rights reserved.

## 1. Introduction

The solubilisation and reconstitution of lipid membranes are of fundamental importance in membrane biochemistry and biophysics. The mechanisms of vesicle dissolution and formation have been widely studied in connection with the solubilisation of biological membranes and the reconstitution of purified, detergent-solubilised membrane proteins into lipid bilayers (for a review, see [1]). The types of detergent and lipid, the detergent/lipid ratio, and the phase state of the detergent/lipid mixture have emerged as key parameters for the functional reconstitution of membrane proteins [1]. Hence, composition-dependent transformations of vesicles into micelles (solubilisation) or *vice versa* (reconstitution) in mixtures of bilayer-forming phospholipids and micelle-forming detergents have received particular attention. The most thoroughly studied detergents include *n*-octyl- $\beta$ -D-glucopyranoside (octylglucoside, OG; [2–6]), Triton X-100 [3,7], 3-[(3-cholamidopropyl)dimethylammonio]-1-propanesulphonate (CHAPS; [8–10]), and other bile acid derivatives [3–5,11,12].

Among the methods traditionally used to monitor solubilisation and reconstitution processes are turbidimetry [2–6,9,11,12], fluorescence resonance energy transfer [2,6,13,14], dynamic light scattering [4,7],

centrifugation followed by quantification of lipid and detergent [15], and electron microscopy [3,7,11,16]. During the last two decades, isothermal titration calorimetry (ITC) has been established as an exceptionally powerful technique for monitoring the composition-dependent phase behaviour of detergent/lipid mixtures (see [12,17–23] for examples, [24,25] for reviews, and [26] for a step-by-step protocol). More recently, it has also been applied to characterising the lipid interactions of lipopeptides with detergent-like properties [27–30].

Many, if not most, of the solubilisation and reconstitution experiments cited above were performed using highly purified egg-yolk phosphatidylcholine (PC) or well-defined synthetic PCs like 1-palmitoyl-2-oleoyl-*sn*-glycero-3-phosphocholine (POPC) as the bilayer-forming species. This is because zwitterionic PCs (of different chain lengths and degrees of saturation) are the major components of the outer leaflets of mammalian cell membranes and thus lend themselves particularly well for the study of mammalian membrane proteins. In one case, the solubilisation behaviour of complex erythrocyte membranes has indeed been shown to be remarkably similar to that of artificial membranes consisting of pure POPC [31]. Furthermore, PCs are available commercially in high purities and at low costs. Thus, the application of ITC to lipid bilayers rich in PC lipids is well-established, and thermodynamic parameters of detergent/lipid interactions and bilayer-to-micelle transitions have been described for a broad spectrum of detergents [12,17–23].

However, many laboratories, including ours, are interested in the reconstitution of bacterial proteins, whose native environments contain a range of phospholipids but no PCs. For instance, the three

\* Corresponding author. Molecular Biophysics, University of Kaiserslautern, Erwin-Schrödinger-Str. 13, 67663 Kaiserslautern, Germany. Tel.: +49 631 205 4908; fax: +49 631 205 4895.

E-mail address: [mail@sandrokeller.com](mailto:mail@sandrokeller.com) (S. Keller).

major phospholipid components of the cytoplasmic membrane of *Escherichia coli* are phosphatidylethanolamine (PE), phosphatidylglycerol (PG), and diphosphatidylglycerol (DPG, also known as cardiolipin), of which PE alone accounts for ~70 mol% of all phospholipid [32,33]. As the functional reconstitution of membrane proteins may crucially depend on the presence of certain lipids or generic membrane properties (such as headgroup charge, degree of acyl chain unsaturation, and lateral pressure profile) imparted by them, it is often desirable to use a lipid mixture that closely resembles the composition of the native membrane. Natural lipid extracts from *E. coli* and other bacterial sources are commercially available and have been employed successfully for the reconstitution of different membrane proteins [34–36], but we are not aware of any publications describing the solubilisation and reconstitution of lipid vesicles composed of such mixtures using ITC.

Here, we report systematic ITC studies of the detergent-mediated solubilisation and reconstitution processes of unilamellar vesicles composed of *E. coli* polar lipid extract. We chose the non-ionic detergent OG because it is one of the most frequently used detergents in the purification and reconstitution of membrane proteins and because its interactions with well-defined lipid systems have been studied in great detail (see references cited above). For comparison with an established lipid system, we present similar experiments for unilamellar vesicles made up of synthetic POPC. For both lipids, we monitored the transitions between bilayer vesicles and micelles with the aid of high-sensitivity ITC, constructed the corresponding phase diagrams displaying the bilayer, bilayer/micelle coexistence, and micellar ranges, and derived the bilayer-to-micelle partition coefficients of both detergent and lipid. Differences in the latter between POPC and *E. coli* polar lipid extract could be explained by differences in the molecular shapes of the constituent lipid species.

## 2. Theory

### 2.1. Solubilisation and reconstitution by ITC

In 1995 and 1996, Blume and co-workers [17,18] established ITC as an accurate and convenient means of monitoring changes in the aggregational state of detergent/lipid mixtures. In solubilisation experiments, these changes arise from a stepwise addition of detergent to lipid, whereas reconstitution experiments proceed in the opposite direction by addition of lipid to detergent. Importantly, structural changes are accompanied by changes in the thermodynamic state of the system and, therefore, can be traced by recording the heats of reaction during titration under isothermal and isobaric conditions.

Solubilisation experiments are performed by titrating lipid vesicles in the ITC sample cell with a micellar detergent solution. In the beginning of the titration, the detergent micelles injected from the syringe disintegrate upon dilution into the sample cell, and detergent monomers partition between the aqueous phase and the bilayer phase. However, the bilayer (b) can accommodate detergent (D) only up to a saturating (SAT) detergent/lipid mole ratio denoted as  $R_D^{b,SAT}$ . Further titration with detergent leads to bilayer dissolution and formation of lipid-saturated micelles, which coexist with detergent-saturated vesicles. To a rather good first approximation known as the phase separation model [37], increasing the detergent concentration in this coexistence range does not affect the compositions of the vesicles and the micelles, but merely raises the number of mixed micelles at the expense of mixed vesicles. Complete solubilisation (SOL) is achieved when the last mixed vesicles disappear at a second characteristic mole ratio denoted as  $R_D^{m,SOL}$ , which gives the minimal detergent/lipid ratio in the micellar (m) phase. Beyond this point, addition of detergent simply increases the detergent/lipid ratio in the mixed micelles, which may, however, undergo another composition-driven transition between different micellar shapes [38].

In reconstitution experiments, by contrast, a micellar detergent solution is titrated with lipid vesicles. In the beginning, the lipid vesicles injected into the sample cell are solubilised completely by the micelles, which decreases the detergent/lipid mole fraction in the micelles. Once  $R_D^{m,SOL}$  is reached, the micelles are saturated with lipid, and detergent-saturated bilayer vesicles begin to coexist with lipid-saturated micelles in the coexistence range. At the  $R_D^{b,SAT}$  boundary, the last mixed micelles disappear, and only mixed vesicles are left.

When following solubilisation (or reconstitution) by ITC, the detergent (or lipid) concentration in the sample cell is increased in a stepwise and fully automated fashion by addition of small aliquots of a concentrated, micellar detergent (or vesicular lipid) suspension from the titration syringe. Each injection brings the detergent/lipid mixture in the cell out of equilibrium. A new equilibrium state is established by the ensuing transfer of lipid and detergent among different aggregational states, which, along the lines of the phase separation model [37], are treated as thermodynamic phases (namely, the aqueous phase, the bilayer phase, and the micellar phase). This process is accompanied by the consumption or release of heat, depending on whether endo- or exothermic processes dominate. In modern compensation-type microcalorimeters, the heat,  $Q$ , is detected as the integral of the power difference between the sample cell and the reference cell,  $\Delta p$ , over time,  $t$ . Plotting the  $Q$  values recorded in solubilisation or reconstitution experiments versus the titrant (detergent or lipid) concentration reveals three ranges characterised by smooth heat traces that are delimited by two points at which  $Q$  changes dramatically within a few injections. Thus, each solubilisation or reconstitution experiment yields one pair of detergent and lipid concentrations marking the SAT boundary and a second pair marking the SOL boundary. Performing several solubilisation and reconstitution experiments at different lipid and detergent concentrations, respectively, furnishes more pairs of detergent and lipid concentrations representing the SAT and SOL boundaries. Plotting the critical detergent concentrations versus the corresponding lipid concentrations finally gives a phase diagram in which a coexistence range is separated from bilayer and micellar ranges by two straight lines corresponding to the SAT and SOL boundaries, respectively.

### 2.2. Equations

The straight lines at the SAT and SOL boundaries are given by the following equations:

$$c_D^{SAT} = c_D^{aq,SAT} + R_D^{b,SAT} c_L, \quad (1)$$

$$c_D^{SOL} = c_D^{aq,SOL} + R_D^{m,SOL} c_L, \quad (2)$$

with  $c_D$  denoting the total detergent concentration,  $c_D^{aq}$  the detergent concentration in the aqueous (aq) phase, and  $c_L$  the total lipid (L) concentration. The slopes of the SAT and SOL boundaries provide the detergent/lipid mole ratios at bilayer saturation,  $R_D^{b,SAT} \equiv c_D^{b,SAT}/c_L$ , and complete vesicle solubilisation,  $R_D^{m,SOL} \equiv c_D^{m,SOL}/c_L$ . The intercepts of the SAT and SOL lines with the y-axis give the concentrations of detergent in the aqueous phase in equilibrium with mixed bilayers and mixed micelles,  $c_D^{aq,SAT}$  and  $c_D^{aq,SOL}$ , respectively. Within the approximation that these supramolecular structures can be treated as thermodynamic phases [37], Gibbs' phase rule requires  $c_D^{aq}$  to be constant throughout the coexistence range, so that  $c_D^{aq,SAT} = c_D^{aq,SOL}$ .

From the threshold mole ratios obtained from the phase diagram, the mole fractions of detergent in coexisting bilayers and micelles are calculated as:

$$x_D^{b,SAT} = R_D^{b,SAT} / (1 + R_D^{b,SAT}), \quad (3)$$

$$X_D^{m,SOL} = R_D^{m,SOL} / (1 + R_D^{m,SOL}). \quad (4)$$

The mole fraction of detergent in the aqueous phase is:

$$X_D^{aq,SAT/SOL} \equiv c_D^{aq,SAT/SOL} / (c_W + c_D^{aq,SAT/SOL}) \approx c_D^{aq,SAT/SOL} / c_W, \quad (5)$$

where the second relationship results from the large excess of water (W) in the aqueous phase,  $c_W = 55.5$  M. The mole fraction partition coefficients of detergent and lipid between detergent-saturated bilayers and lipid-saturated micelles then read:

$$K_L^{m/b} \equiv X_L^{m,SOL} / X_L^{b,SAT} = (1 - X_D^{m,SOL}) / (1 - X_D^{b,SAT}), \quad (6)$$

$$K_D^{m/b} \equiv X_D^{m,SOL} / X_D^{b,SAT}. \quad (7)$$

Finally, the detergent partition coefficients between the aqueous phase and detergent-saturated bilayers and lipid-saturated micelles are, respectively:

$$K_D^{b/aq} \equiv X_D^{b,SAT} / X_D^{aq,SAT/SOL} \quad (8)$$

$$K_D^{m/aq} \equiv X_D^{m,SOL} / X_D^{aq,SAT/SOL}. \quad (9)$$

### 3. Materials and methods

#### 3.1. Materials

Synthetic POPC was purchased from Genzyme Pharmaceuticals (Liestal, Switzerland). *E. coli* polar lipid extract was obtained from Avanti Polar Lipids (Alabaster, USA). According to the manufacturer's specifications ([http://avantilipids.com/index.php?option=com\\_content&view=article&id=409&Itemid=124&catnumber=100600](http://avantilipids.com/index.php?option=com_content&view=article&id=409&Itemid=124&catnumber=100600)), the lipid composition of the extract was 67.0% PE, 23.2% PG, and 9.8% DPG. OG was from Glycon Biochemicals (Luckenwalde, Germany), and buffer components were purchased from Carl Roth (Karlsruhe, Germany). All chemicals were obtained in the highest available purities. All experiments were performed in 10 mM potassium phosphate buffer ( $KH_2PO_4/K_2HPO_4$ ) containing 150 mM KF and adjusted to pH 7.1.

#### 3.2. Vesicle preparation

Unilamellar vesicles composed of POPC or *E. coli* polar lipid extract were prepared by extrusion or sonication, respectively. First, dry lipid powder was suspended in buffer by vortexing for 20 min. Then, POPC vesicles were prepared by 35 extrusion steps through two stacked polycarbonate filters with 100-nm pores using a MiniExtruder (Avestin, Ottawa, Canada). By contrast, *E. coli* lipid vesicles were made by sonication of the lipid suspension for 40 min using a Sonopuls instrument (Bandelin Electronic, Berlin, Germany) at 30% power level. During sonication, the lipid suspension was cooled in an ice/water bath and purged with  $N_2$ . Vesicle sizes were found to be narrowly centred at 100 nm for POPC and 80 nm for *E. coli* lipid vesicles, as determined by dynamic light scattering performed on a Zetasizer NanoSZ device (Malvern Instruments, Worcestershire, UK). We chose different methods of vesicle preparation because sonication of POPC leads to much smaller vesicles (~30 nm in diameter), whereas extrusion of *E. coli* lipid is difficult and does not result in a unimodal size distribution below 200 nm. Using different preparation methods, we could achieve similar vesicle sizes, which we considered more important than using the same method. For the *E. coli* polar lipid extract, we assumed an average molar mass of 700 g/mol.

#### 3.3. Isothermal titration calorimetry

High-sensitivity ITC was performed on a VP-ITC instrument (GE Healthcare, Uppsala, Sweden) after vacuum degassing of the samples. Solubilisation and reconstitution titrations were carried out essentially as described elsewhere [26]. For solubilisation, small aliquots of a concentrated detergent solution (100 mM) were injected into the ITC sample cell containing lipid vesicles (1–6.5 mM) and a submicellar concentration of OG (16–21 mM). Premixing the lipid with OG in the cell was necessary to cross both the SAT and the SOL boundaries in one titration without refilling the injection syringe. For reconstitution, lipid suspensions (40–50 mM) were injected into the sample cell filled with a micellar detergent suspension (30–36 mM). The injection volumes ranged from 1  $\mu$ L to 5  $\mu$ L, which is at the lower limit recommended for this calorimeter model. In our experience, however, such small injections did not pose any problems, as the reproducibility was excellent and the results did not depend on the injection volumes, arguing against a noticeable influence of diffusive leakage from the syringe tip during the long re-equilibration times required. The critical micellar concentration (CMC) of OG under the conditions used was found to be 29.6 mM, as obtained from ITC demicellisation experiments (data not shown, see [22] for an example). All experiments were performed at 8 °C because this is the temperature of choice for the reconstitution of several bacterial membrane proteins.

The time spacings between injections were chosen long enough to allow for nearly complete re-equilibration of the system (12–15 min). Baseline subtraction and peak integration were accomplished using Origin 7 as described by the manufacturer (OriginLab, Northampton, USA). Reaction heats were normalised with respect to the molar amount of titrant (detergent or lipid) injected. The first injection was always excluded from presentation (see Figs. 1, 2, 4, and 5) because it usually suffers from sample loss during the mounting of the syringe and the equilibration preceding the actual titration. Phase boundaries were identified by determining the pairs of detergent and lipid concentrations at the inflection points of the integrated heat values. Inflection points were obtained as the maxima and minima in the first derivative of the integrated heat with respect to the titrant (detergent or lipid) concentration.

### 4. Results

ITC solubilisation and reconstitution experiments were carried out to monitor composition-dependent changes in the aggregational state of mixtures of OG with either synthetic POPC or *E. coli* polar lipid extract and to derive the corresponding partition coefficients and phase diagrams.

#### 4.1. POPC

We first examined the OG-driven solubilisation of unilamellar vesicles composed of synthetic POPC. Fig. 1 depicts the raw data (A) and the integrated heats of reaction (B) obtained upon injecting 100 mM OG into 2 mM POPC vesicles premixed with 19 mM OG. The integrated and normalised heats of reaction,  $Q_D$ , reveal three distinct ranges as a function of detergent concentration,  $c_D$ . The  $Q_D$  values change smoothly within each of these ranges but rise or drop abruptly at the boundaries separating them. In the illustrated titration, dramatic changes occur at detergent concentrations of  $c_D = 22$  mM and  $c_D = 24$  mM when the system crosses the SAT and SOL boundaries, respectively. Hence, the three intervals displaying continuous  $Q_D$  traces can be ascribed to the bilayer, the coexistence, and the micellar ranges. Within the bilayer range, exothermic heats of reaction stem from micelle disintegration and detergent partitioning into bilayer vesicles. In the coexistence range, solubilisation takes place, but the bilayer-to-micelle transfer heats of lipid and detergent nearly cancel each other, resulting in small absolute  $Q_D$  values. In the

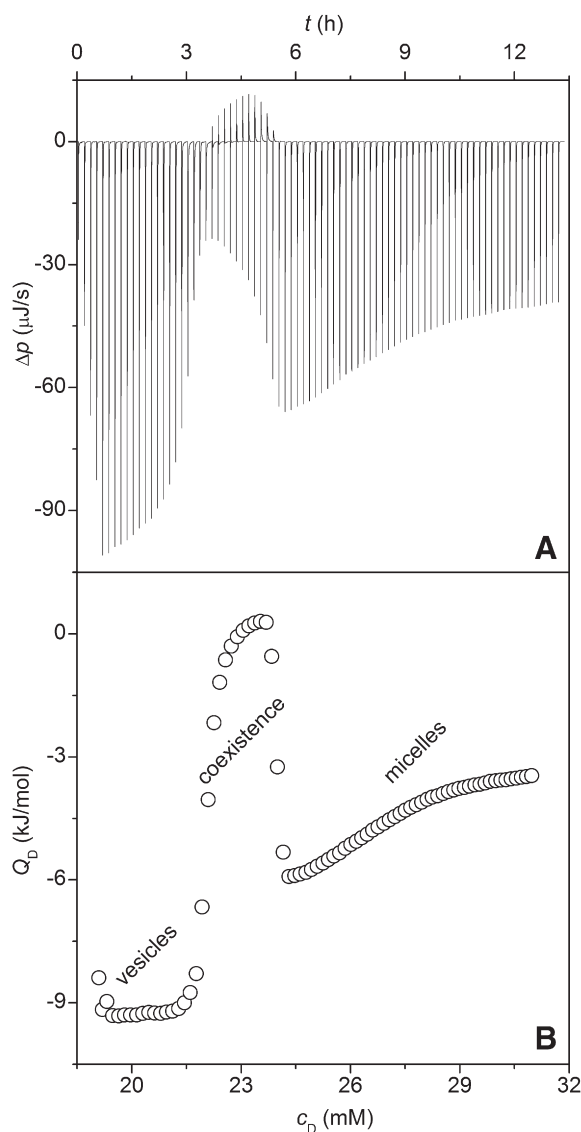


**Fig. 1.** Solubilisation of POPC vesicles at 8 °C. 100 mM OG was titrated into 2 mM POPC and 19 mM OG. (A) Differential heating power,  $\Delta p$ , versus time,  $t$ . (B) Integrated and normalised heat of reaction,  $Q_D$ , versus total detergent concentration in the ITC sample cell,  $c_D$ . Injection volumes were 1.0, 1.5, 2.0, 2.5, and  $76 \times 3.0$   $\mu\text{L}$ .

micellar range, further addition of detergent leads to micelle disintegration, whose exothermic effect decreases in magnitude as the aqueous detergent concentration approaches the CMC.

A representative experiment demonstrating the reconstitution of POPC vesicles is given in Fig. 2. Here, a 30 mM solution of OG was titrated with 40 mM POPC vesicles. Again, three ranges are obvious when plotting  $Q_L$  against the lipid concentration,  $c_L$ . The SOL and SAT boundaries appear at  $c_L = 3.3$  mM and  $c_L = 5.5$  mM, respectively. In the micellar range, endothermic  $Q_L$  values are due to vesicle solubilisation and, possibly, a transition between different micellar shapes as the lipid concentration increases [38]. In the coexistence range, reconstitution sets in, but the micelle-to-bilayer transfer heats of lipid and detergent again cancel one another to a large extent. In the bilayer range, further addition of lipid entails detergent partitioning from the aqueous phase, which is accompanied by endothermic heats of reaction.

We performed solubilisation and reconstitution experiments for a number of other initial lipid and detergent concentrations, respectively. The phase diagram in Fig. 3 was obtained by plotting the

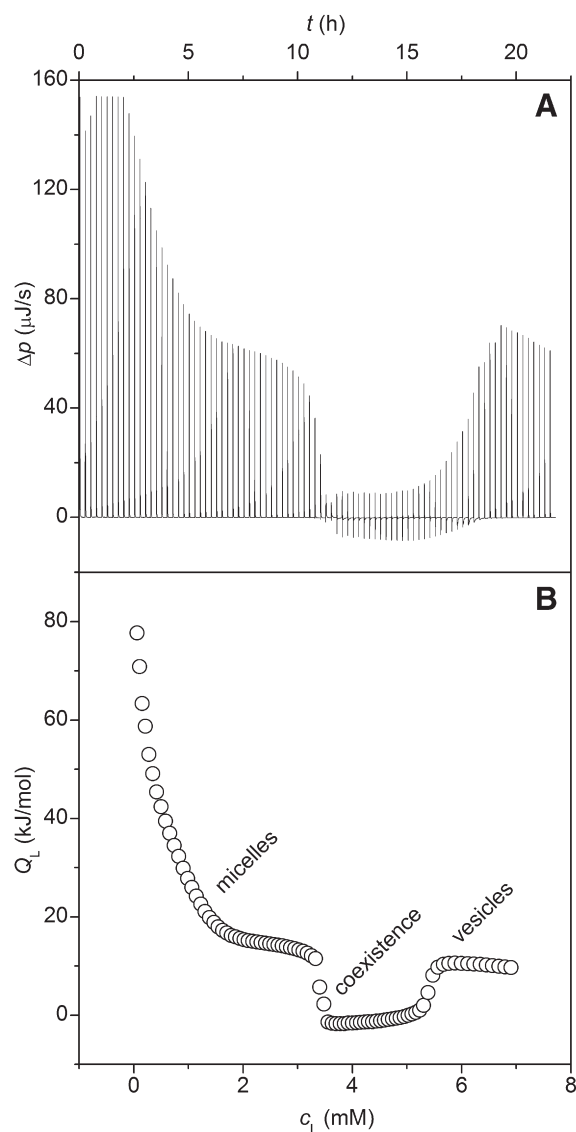


**Fig. 2.** Reconstitution of POPC vesicles at 8 °C. 40 mM POPC was titrated into 30 mM OG. (A) Differential heating power,  $\Delta p$ , versus time,  $t$ . (B) Integrated and normalised heat of reaction,  $Q_L$ , versus total lipid concentration in the ITC sample cell,  $c_L$ . Injection volumes were  $2 \times 1.5$ , 1.7, 2.0, 2.2, 2.4, 2.6, 2.8,  $64 \times 3.0$ ,  $3.5$ ,  $2 \times 4.0$ ,  $2 \times 4.5$ , and  $10 \times 5.0$   $\mu\text{L}$ .

detergent concentrations at the SAT and SOL boundaries versus the corresponding lipid concentrations. Fitting the SAT and SOL data with the aid of Eqs. (1) and (2), respectively, while assuming a common y-axis intercept for both linear regressions yielded  $c_D^{\text{aq-SAT/SOL}} = 19.6$  mM,  $R_D^{\text{b-SAT}} = 1.22$ , and  $R_D^{\text{m-SOL}} = 2.38$ . Thus, POPC vesicles can incorporate up to 1.2 OG molecules per lipid molecule before solubilisation sets in, whereas mixed micelles must contain at least 2.4 OG molecules per POPC molecule. In the coexistence range, the concentration of free detergent is 19.6 mM, which is substantially lower than the CMC of 29.6 mM because, in the presence of lipid, the monomeric detergent in the aqueous phase is in equilibrium with lipid-saturated mixed micelles rather than pure detergent micelles.

#### 4.2. E. coli polar lipid extract

In a second set of experiments, we performed solubilisation and reconstitution titrations using unilamellar vesicles consisting of *E. coli* polar lipid extract. Figs. 4 and 5 exemplify the processes of vesicle solubilisation and reconstitution, respectively. Both titrations are



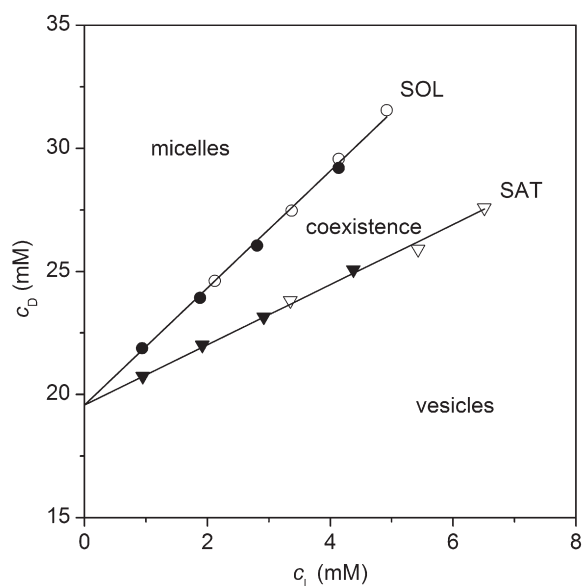


**Fig. 3.** Phase diagram of OG/POPC mixtures at 8 °C. Triangles and circles denote the SAT and SOL boundaries, respectively. Solid symbols are from solubilisation experiments, whereas open symbols are from reconstitution experiments. Straight lines are fits of the SAT and SOL boundaries according to Eqs. (1) and (2), respectively; fitting parameters are given in Table 1.

qualitatively similar to the corresponding experiments using POPC vesicles, though quantitative differences can be observed. Here too, the titrations are characterised by three ranges separated by two events ascribed to the SAT and SOL boundaries. The most obvious difference is the width of the coexistence range, which is substantially broader for *E. coli* lipid than for POPC.

This becomes more obvious in the phase diagram depicted in Fig. 6. The phase boundaries are now described by  $c_D^{\text{aq,SAT/SOL}} = 23.4$  mM,  $R_D^{\text{b,SAT}} = 0.947$ , and  $R_D^{\text{m,SOL}} = 3.11$ . Hence, *E. coli* vesicles can incorporate a maximum of only 0.95 OG molecules per lipid molecule. Nevertheless, when compared with POPC vesicles, more detergent is required for complete solubilisation of *E. coli* lipid vesicles, as mixed micelles must contain at least 3.1 OG molecules per lipid molecule. The concentration of free detergent in equilibrium with lipid-saturated mixed micelles is 23.4 mM, which is also higher than in the case of POPC.

## 5. Discussion

ITC has previously been shown to be an excellent tool for studying the interactions of detergents with bilayer membranes made up of well-defined lipids or lipid mixtures (see most of the references cited in this paper) or lipid extracts derived from mammalian membranes [31]. The present report demonstrates that ITC is applicable to studying such interactions involving lipid mixtures extracted from bacterial sources such as *E. coli* membranes, which differ dramatically in their lipid composition from mammalian membranes.

The OG-driven solubilisation and reconstitution processes of POPC and *E. coli* lipid vesicles can be explained by the three-stage phase separation model [37] previously applied to a range of simple detergent/lipid systems. For the *E. coli* polar lipid extract, such a simple behaviour could not be taken for granted *a priori*. On the one hand, the solubilisation and reconstitution of lipid mixtures may follow a complex pattern, as detergents might preferentially solubilise certain lipids or induce lipid demixing [39,40]. Gibbs' phase rule postulates that the maximal number of coexisting phases in a three-component system (such as water, lipid, and detergent) is three. In a system containing

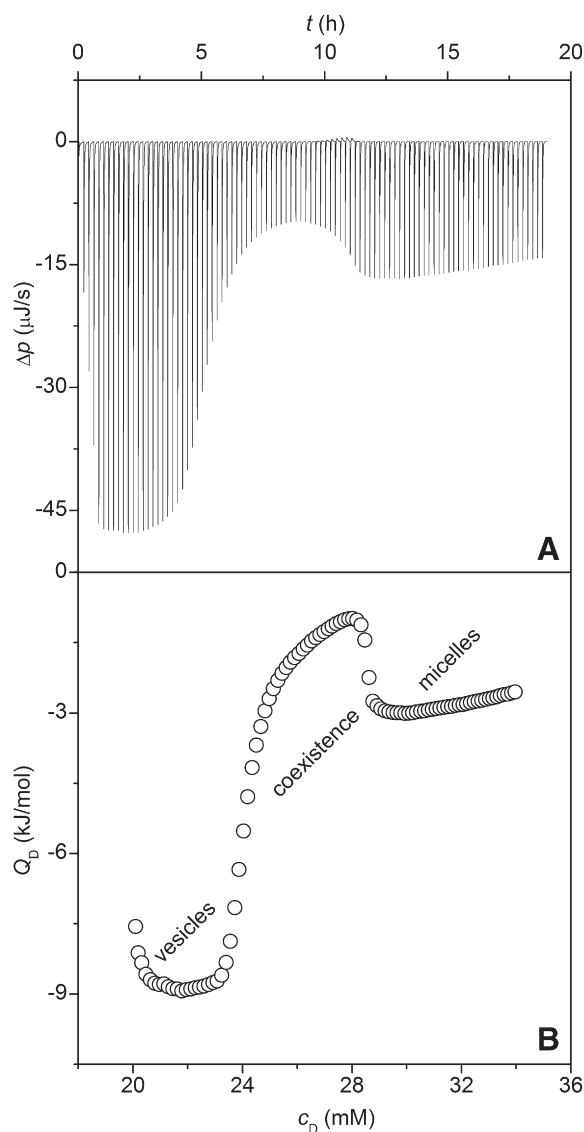


**Fig. 4.** Solubilisation of vesicles composed of *E. coli* polar lipid extract at 8 °C. 100 mM OG was titrated into 2 mM *E. coli* lipid and 20 mM OG. (A) Differential heating power,  $\Delta p$ , versus time,  $t$ . (B) Integrated and normalised heat of reaction,  $Q_D$ , versus total detergent concentration in the ITC sample cell,  $c_D$ . Injection volumes were 1.0, 1.5, 2.0, 2.5, and  $76 \times 3.0$   $\mu$ L.

more components (for instance, additional lipid species), the number of coexisting phases could increase accordingly. However, we found that the solubilisation and reconstitution processes of vesicles made from *E. coli* polar lipid extract display no qualitative differences when compared with those of simpler systems; thus, they can be rationalised without invoking additional coexisting phases (such as different types of micelles, vesicles, or membrane domains). On the other hand, even the solubilisation and reconstitution of bilayers made up of a single phospholipid component may unveil a picture that is not compatible with the three-stage phase separation model. For example, Blume and co-workers [20] obtained phase diagrams for mixtures of OG and different PCs in which the SAT and SOL lines markedly differ in their y-axis intercepts, suggesting systematic errors in determining the SAT and SOL boundaries or a slight increase in the free detergent concentration,  $c_D^{\text{aq}}$ , within the coexistence range. We encountered neither problem, as fitting the SAT and SOL boundaries with independently adjustable  $c_D^{\text{aq,SAT}}$  and  $c_D^{\text{aq,SOL}}$  parameters yielded values virtually identical to those listed in Table 1. Moreover, our  $R_D^{\text{b,SAT}}$  and  $R_D^{\text{m,SOL}}$

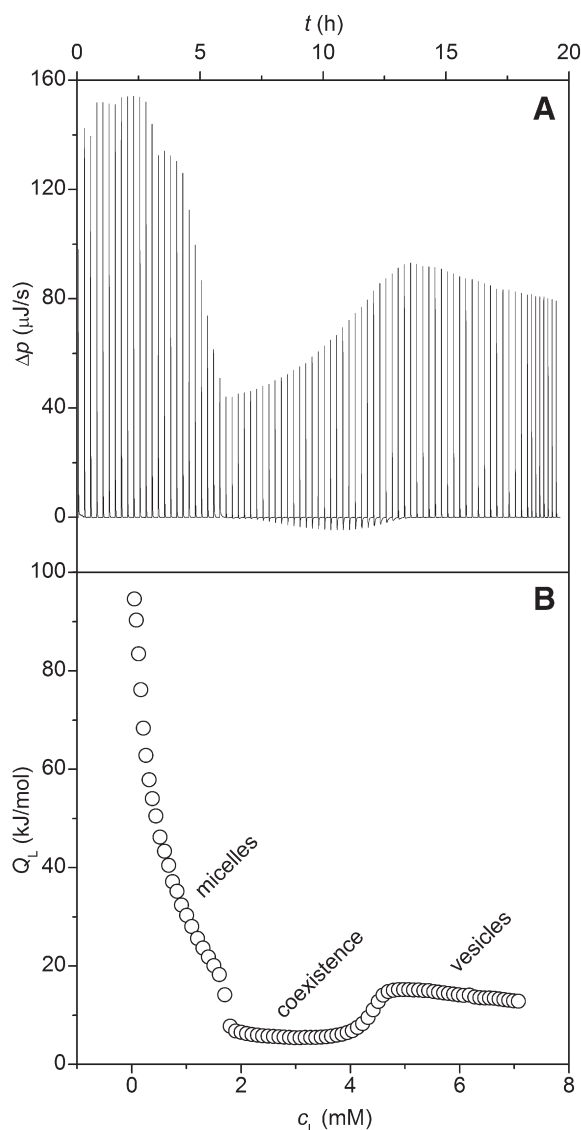


**Fig. 5.** Reconstitution of vesicles composed of *E. coli* polar lipid extract at 8 °C. 50 mM *E. coli* lipid was titrated into 30 mM OG. (A) Differential heating power,  $\Delta p$ , versus time,  $t$ . (B) Integrated and normalised heat of reaction,  $Q_L$ , versus total lipid concentration in the ITC sample cell,  $c_L$ . Injection volumes were  $3 \times 1.0, 1.2, 1.3, 1.4, 1.5, 1.7, 1.8, 2.0, 4 \times 2.2, 2.4, 2.6, 2.8$ , and  $64 \times 3.0$   $\mu\text{L}$ .

values for the OG/POPC system are in good agreement with previously reported data [23,41].

The ITC titrations employing POPC and *E. coli* polar lipid extract revealed similar overall patterns on the qualitative level (compare Figs. 1 and 4 as well as Figs. 2 and 5), but quantitative differences became apparent on plotting the phase diagrams (compare Figs. 3 and 6). Most notable is a considerable widening of the coexistence range for *E. coli* polar lipid extract when compared with POPC, as has been reported for soybean PC in comparison with synthetic PCs possessing saturated acyl chains [20]. In the present case, this widening is due to both a decrease in  $R_D^{b,\text{SAT}}$  and an increase in  $R_D^{m,\text{SOL}}$  (see Table 1). Thus, solubilisation commences at a lower but is completed at a higher detergent content in the mixed detergent/lipid aggregates (bilayers and micelles). To rationalise this finding, it is important to realise that  $R_D^{b,\text{SAT}}$  and  $R_D^{m,\text{SOL}}$  are determined by the bilayer-to-micelle partition coefficients of the lipid,  $K_L^{m/b}$ , and the detergent,  $K_D^{m/b}$ . It is intuitively clear that increasing the affinity of the lipid or the detergent for the micellar phase will facilitate micelle formation, that is, decrease both  $R_D^{b,\text{SAT}}$  and  $R_D^{m,\text{SOL}}$ .

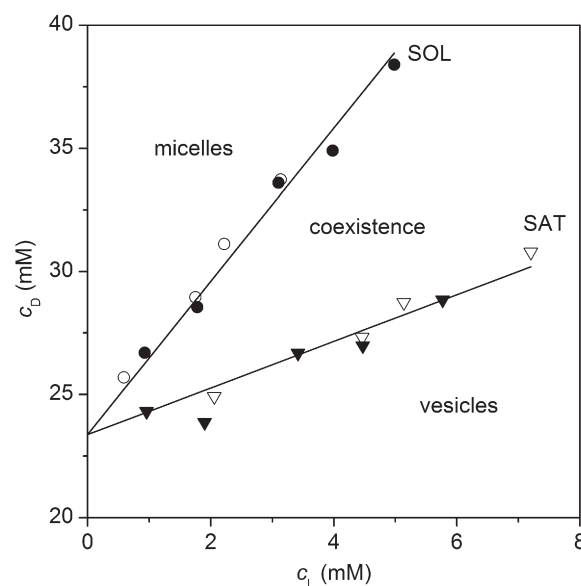


**Fig. 6.** Phase diagram of OG/*E. coli* polar lipid extract mixtures at 8 °C. Triangles and circles denote the SAT and SOL boundaries, respectively. Solid symbols are from solubilisation experiments, whereas open symbols are from reconstitution experiments. Straight lines are fits of the SAT and SOL boundaries according to Eqs. (1) and (2), respectively; fitting parameters are given in Table 1.

Quantitatively, this is expressed by solving Eqs. (3), (4), (6) and (7) for the critical mole ratios, which are given by:

$$R_D^{b,\text{SAT}} = (1 - K_L^{m/b}) / (K_D^{m/b} - 1), \quad (10)$$

$$R_D^{m,\text{SOL}} = K_D^{m/b} / K_L^{m/b} (1 - K_L^{m/b}) / (K_D^{m/b} - 1) = K_D^{m/b} / K_L^{m/b} \times R_D^{b,\text{SAT}}. \quad (11)$$

As expected,  $R_D^{b,\text{SAT}}$  and  $R_D^{m,\text{SOL}}$  decrease as either  $K_L^{m/b}$  or  $K_D^{m/b}$  increases while keeping the other partition coefficient constant. Moreover, Eqs. (10) and (11) predict that a decrease in  $R_D^{b,\text{SAT}}$  and a concomitant increase in  $R_D^{m,\text{SOL}}$ , as observed on replacing POPC by *E. coli* lipid, can result only from a drop in  $K_L^{m/b}$  and a simultaneous rise in  $K_D^{m/b}$ .

The bilayer-to-micelle partition coefficients calculated with the aid of Eqs. (6) and (7) are also given in Table 1.  $K_L^{m/b} < 1$  and  $K_D^{m/b} > 1$  irrespective of the lipid system used, reflecting the fact that the lipids prefer the bilayer phase over the micellar phase, while the opposite is true for the detergent. In the case in hand, replacing POPC by *E. coli* polar lipid extract reduces  $K_L^{m/b}$  from 0.66 to 0.47. The attenuated affinity of the lipid for the micellar phase versus the bilayer phase can be explained by the high PE content (~70 mol%) in the *E. coli* lipid mixture. Unsaturated PEs have a negative spontaneous curvature [42,43], that is, their headgroups occupy considerably less area than their acyl chains do, rendering their transfer into highly positively curved, micellar structures unfavourable (the same holds for DPG in the presence of  $\text{Ca}^{2+}$ ). By contrast, because of its rather cylindrical shape, POPC has almost no spontaneous curvature [43] and is therefore less reluctant to partition into micelles. At the same time,

**Table 1**

Parameters describing the OG-driven solubilisation and reconstitution of lipid vesicles composed of either synthetic POPC or *E. coli* polar lipid extract at 8 °C in 10 mM  $\text{KH}_2\text{PO}_4/\text{K}_2\text{HPO}_4$ , 150 mM KF, pH 7.1.

Lipid	$c_D^{\text{aq,SAT/SOL}}$ (mM)	$R_D^{b,\text{SAT}}$	$R_D^{m,\text{SOL}}$	$X_D^{b,\text{SAT}}$	$X_D^{m,\text{SOL}}$	$K_L^{m/b}$	$K_D^{m/b}$	$K_B^{b/aq}$ ( $10^3$ )	$K_B^{m/aq}$ ( $10^3$ )
POPC	19.6	1.22	2.38	0.55	0.70	0.66	1.3	1.6	2.0
<i>E. coli</i> lipid	23.4	0.947	3.11	0.49	0.76	0.47	1.6	1.2	1.8

$K_D^{m/b}$  increases from 1.3 to 1.6, indicating that the detergent's preference for the micellar phase over the bilayer phase becomes more pronounced as POPC is replaced by *E. coli* polar lipid extract. PE condenses lipid bilayers and increases the core lateral pressure [44], which hampers insertion of OG monomers. This is also borne out by the water-to-bilayer partition coefficient,  $K_D^{b/aq}$ , which decreases more strongly than the water-to-micelle partition coefficient,  $K_D^{m/aq}$ , upon substitution of POPC by *E. coli* lipid (see Table 1).

Another major difference between the lipids used in this work lies in their acyl chain compositions. Whereas POPC has a fully saturated C16 and a singly unsaturated C18 chain, the *E. coli* lipid mixture contains a wide spectrum of different fatty acyl chains, including also shorter and branched ones [32]. This peculiar combination of different acyl chains with different headgroups is expected to affect the partition coefficients and phase boundaries, too, but a less speculative account must await a more accurate knowledge of the lipid composition.

In summary, the present report shows that the OG-mediated solubilisation and reconstitution processes of unilamellar vesicles composed of a complex lipid mixture extracted from *E. coli* membranes can be described reasonably well by the three-stage phase separation model. Quantitative differences as compared with POPC bilayers may be traced back to the high content of lipids with negative spontaneous curvature in the *E. coli* polar lipid extract.

## Acknowledgements

We thank Prof. Heiko Heerklotz (Leslie Dan Faculty of Pharmacy, University of Toronto, Canada) and Dr. Carolyn Vargas (Molecular Biophysics, University of Kaiserslautern, Germany) for numerous stimulating discussions and Monika Georgi (Leibniz Institute of Molecular Pharmacology (FMP), Berlin, Germany) for excellent technical assistance.

## References

- [1] J.L. Rigaud, B. Pitard, D. Levy, Reconstitution of membrane proteins into liposomes: application to energy-transducing membrane proteins, *Biochim. Biophys. Acta* 1231 (1995) 223–246.
- [2] M. Ollivon, O. Eidelman, R. Blumenthal, A. Walter, Micelle-vesicle transition of egg phosphatidylcholine and octyl glucoside, *Biochemistry* 27 (1988) 1695–1703.
- [3] M.T. Paternostre, M. Roux, J.L. Rigaud, Mechanisms of membrane protein insertion into liposomes during reconstitution procedures involving the use of detergents. 1. Solubilization of large unilamellar liposomes (prepared by reverse-phase evaporation) by Triton X-100, octyl glucoside, and sodium cholate, *Biochemistry* 27 (1988) 2668–2677.
- [4] S. Almog, B.J. Litman, W. Wimley, J. Cohen, E.J. Wachtel, Y. Barenholz, A. Ben Shaul, D. Lichtenberg, States of aggregation and phase transformations in mixtures of phosphatidylcholine and octyl glucoside, *Biochemistry* 29 (1990) 4582–4592.
- [5] C.H. Spink, V. Lieto, E. Mereand, C. Pruden, Micelle-vesicle transition in phospholipid-bile salt mixtures. A study by precision scanning calorimetry, *Biochemistry* 30 (1991) 5104–5112.
- [6] M. Paternostre, O. Meyer, C. Grabielle-Madellmont, S. Lesieur, M. Ghanam, M. Ollivon, Partition coefficient of a surfactant between aggregates and solution: application to the micelle-vesicle transition of egg phosphatidylcholine and octyl- $\beta$ -D-glucopyranoside, *Biophys. J.* 69 (1995) 2476–2488.
- [7] O. López, A. de la Maza, L. Coderch, C. López-Iglesias, E. Wehrli, J.L. Parra, Direct formation of mixed micelles in the solubilization of phospholipid liposomes by Triton X-100, *FEBS Lett.* 426 (1998) 314–318.
- [8] T. Schürholz, Critical dependence of the solubilization of lipid vesicles by the detergent CHAPS on the lipid composition. Functional reconstitution of the nicotinic acetylcholine receptor into preformed vesicles above the critical micellization concentration, *Biophys. Chem.* 58 (1996) 87–96.
- [9] J. Cladera, J.L. Rigaud, J. Villaverde, M. Dunach, Liposome solubilization and membrane protein reconstitution using Chaps and Chapso, *Eur. J. Biochem.* 243 (1997) 798–804.
- [10] A. Viriyaraj, H. Kashiwagi, M. Ueno, Process of destruction of large unilamellar vesicles by a zwitterionic detergent, CHAPS: partition behavior between membrane and water phases, *Chem. Pharm. Bull.* 53 (2005) 1140–1146.
- [11] A. Walter, P.K. Vinson, A. Kaplun, Y. Talmon, Intermediate structures in the cholate-phosphatidylcholine vesicle-micelle transition, *Biophys. J.* 60 (1991) 1315–1325.
- [12] P. Garidel, A. Hildebrand, K. Knauf, A. Blume, Membranolytic activity of bile salts: influence of biological membrane properties and composition, *Molecules* 12 (2007) 2292–2326.
- [13] O. Eidelman, R. Blumenthal, A. Walter, Composition of octyl glucoside-phosphatidylcholine mixed micelles, *Biochemistry* 27 (1988) 2839–2846.
- [14] K. Andrieux, L. Forte, S. Lesieur, M. Paternostre, M. Ollivon, C. Grabielle-Madellmont, Insertion and partition of sodium taurocholate into egg phosphatidylcholine vesicles, *Pharm. Res.* 21 (2004) 1505–1516.
- [15] M.L. Jackson, C.F. Schmidt, D. Lichtenberg, B.J. Litman, A.D. Albert, Solubilization of phosphatidylcholine bilayers by octyl glucoside, *Biochemistry* 21 (1982) 4576–4582.
- [16] P.K. Vinson, Y. Talmon, A. Walter, Vesicle-micelle transition of phosphatidylcholine and octyl glucoside elucidated by cryo-transmission electron microscopy, *Biophys. J.* 56 (1989) 669–681.
- [17] H. Heerklotz, G. Lantzsch, H. Binder, G. Klose, A. Blume, Application of isothermal titration calorimetry for detecting lipid-membrane solubilization, *Chem. Phys. Lett.* 235 (1995) 517–520.
- [18] H. Heerklotz, G. Lantzsch, H. Binder, G. Klose, A. Blume, Thermodynamic characterization of dilute aqueous lipid/detergent mixtures of POPC and C<sub>12</sub>EO<sub>8</sub> by means of isothermal titration calorimetry, *J. Phys. Chem.* 100 (1996) 6764–6774.
- [19] H. Heerklotz, H. Binder, G. Lantzsch, G. Klose, A. Blume, Lipid/detergent interaction thermodynamics as a function of molecular shape, *J. Phys. Chem. B* 101 (1997) 639–645.
- [20] M. Keller, A. Kerth, A. Blume, Thermodynamics of interaction of octyl glucoside with phosphatidylcholine vesicles: partitioning and solubilization as studied by high sensitivity titration calorimetry, *Biochim. Biophys. Acta* 1326 (1997) 178–192.
- [21] E. Opatowski, D. Lichtenberg, M.M. Kozlov, The heat of transfer of lipid and surfactant from vesicles into micelles in mixtures of phospholipid and surfactant, *Biophys. J.* 73 (1997) 1458–1467.
- [22] S. Keller, H. Heerklotz, N. Jahnke, A. Blume, Thermodynamics of lipid membrane solubilization by sodium dodecyl sulfate, *Biophys. J.* 90 (2006) 4509–4521.
- [23] A. Beck, A.D. Tsamaloukas, P. Jurcevic, H. Heerklotz, Additive action of two or more solutes on lipid membranes, *Langmuir* 24 (2008) 8833–8840.
- [24] H. Heerklotz, J. Seelig, Titration calorimetry of surfactant-membrane partitioning and membrane solubilization, *Biochim. Biophys. Acta* 1508 (2000) 69–85.
- [25] H. Heerklotz, in: G. Cevc (Ed.), *Phospholipids Handbook*, 2nd Edition, III/1 Lipid-Surfactant Interactions, 2006.
- [26] H. Heerklotz, A.D. Tsamaloukas, S. Keller, Monitoring detergent-mediated solubilization and reconstitution of lipid membranes by isothermal titration calorimetry, *Nat. Protoc.* 4 (2009) 686–697.
- [27] H. Heerklotz, J. Seelig, Detergent-like action of the antibiotic peptide surfactin on lipid membranes, *Biophys. J.* 81 (2001) 1547–1554.
- [28] S. Keller, I. Sauer, H. Strauss, K. Gast, M. Dathe, M. Bienenert, Membrane-mimetic nanocarriers formed by a dipalmitoylated cell-penetrating peptide, *Angew. Chem. Int. Ed.* 44 (2005) 5252–5255.
- [29] I. Sauer, H. Nikolenko, S. Keller, K. Abu Ajaj, M. Bienenert, M. Dathe, Dipalmitoylation of a cellular uptake-mediating apolipoprotein E-derived peptide as a promising modification for stable anchorage in liposomal drug carriers, *Biochim. Biophys. Acta* 1758 (2006) 552–561.
- [30] H. Heerklotz, J. Seelig, Leakage and lysis of lipid membranes induced by the lipopeptide surfactin, *Eur. Biophys. J.* 36 (2007) 305–314.
- [31] H. Heerklotz, Interactions of surfactants with lipid membranes, *Q. Rev. Biophys.* 41 (2008) 205–264.
- [32] S. Morein, A. Andersson, L. Rilfors, G. Lindblom, Wild-type *Escherichia coli* cells regulate the membrane lipid composition in a “window” between gel and non-lamellar structures, *J. Biol. Chem.* 271 (1996) 6801–6809.
- [33] W. Dowhan, Molecular basis for membrane phospholipid diversity: why are there so many lipids? *Annu. Rev. Biochem.* 66 (1997) 199–232.
- [34] P. Pohl, S.M. Saparov, M.J. Borgnia, P. Agre, Highly selective water channel activity measured by voltage clamp: analysis of planar lipid bilayers reconstituted with purified AqpZ, *Proc. Natl. Acad. Sci. USA* 98 (2001) 9624–9629.
- [35] S.M. Saparov, D. Kozono, U. Rothe, P. Agre, P. Pohl, Water and ion permeation of aquaporin-1 in planar lipid bilayers. Major differences in structural determinants and stoichiometry, *J. Biol. Chem.* 276 (2001) 31515–31520.
- [36] S.M. Saparov, S.P. Tsunoda, P. Pohl, Proton exclusion by an aquaglyceroprotein: a voltage clamp study, *Biol. Cell* 97 (2005) 545–550.
- [37] D. Lichtenberg, R.J. Robson, E.A. Dennis, Solubilization of phospholipids by detergents: structural and kinetic aspects, *Biochim. Biophys. Acta* 737 (1983) 285–304.
- [38] H. Heerklotz, A. Tsamaloukas, K. Kita-Tokarczyk, P. Strunz, T. Gutberlet, Structural, volumetric, and thermodynamic characterization of a micellar sphere-to-rod transition, *J. Am. Chem. Soc.* 126 (2004) 16544–16552.
- [39] H. Heerklotz, H. Szadkowska, T. Anderson, J. Seelig, The sensitivity of lipid domains to small perturbations demonstrated by the effect of Triton, *J. Mol. Biol.* 329 (2003) 793–799.
- [40] S. Keller, A. Tsamaloukas, H. Heerklotz, A quantitative model describing the selective solubilization of membrane domains, *J. Am. Chem. Soc.* 127 (2005) 11469–11476.
- [41] A. Walter, G. Kuehl, K. Barnes, G. VanderWaerd, The vesicle-to-micelle transition of phosphatidylcholine vesicles induced by nonionic detergents: effects of sodium chloride, sucrose and urea, *Biochim. Biophys. Acta* 1508 (2000) 20–33.
- [42] J.N. Israelachvili, D.J. Mitchell, B.W. Ninham, Theory of self-assembly of lipid bilayers and vesicles, *Biochim. Biophys. Acta* 470 (1977) 185–201.
- [43] P.R. Cullis, B. de Kruijff, Lipid polymorphism and the functional roles of lipids in biological membranes, *Biochim. Biophys. Acta* 559 (1979) 399–420.
- [44] R.A. Demel, B. de Kruijff, The function of sterols in membranes, *Biochim. Biophys. Acta* 457 (1976) 109–132.